Gas-Permeation Properties of Poly(ethylene oxide) Poly(butylene terephthalate) Block Copolymers

S. J. Metz, M. H. V. Mulder, and M. Wessling*

Membrane Technology Group, Faculty of Science and Technology, University of Twente, P.O. Box 217, 7500 AE Enschede, The Netherlands

Received January 22, 2004; Revised Manuscript Received April 20, 2004

ABSTRACT: This paper reports the gas-permeation properties of poly(ethylene oxide) (PEO) poly(butylene terephthalate) (PBT) segmented multiblock copolymers. These block copolymers allow a precise structural modification by the amount of PBT and the PEO segment length, enabling a systematic study of the relationship between polymer composition and morphology and gas-transport properties. The CO_2 and N_2 permeability strongly varies with the amount of PEO and the PEO segment length. The permeabilities are compared to predictions of the Maxwell model, which considers the PBT phase as impermeable. The difference between the experimental values and the Maxwell model are interpreted on the basis of chain flexibility of the PEO phase. The chain flexibility decreases with increasing amounts of PBT due to a less pronounced phase separation between the PEO and PBT phase. This is reflected in an increasing glass-transition temperature of the amorphous PEO phase. The increase of the permeability with an increasing PEO block length, at the same ratio PEO−PBT, can therefore be related to a larger chain flexibility for longer PEO segments. The permeability also depends on the degree of crystallinity and the melting temperature of the PEO phase, which increases with the amount and the PEO segment length. PEO−PBT block copolymers exhibit a high CO_2/N_2selectivity ($\alpha \approx 60$ at $T = 35$ °C) due to the high solubility of CO_2 in the PEO phase. However, this selectivity is structure-dependent and is higher for block copolymers with larger amounts of PBT. The CO_2/He selectivity shows a different structure dependency since the permeation of CO_2 occurs primarily through the PEO phase and the He permeation occurs through both the PEO and mixed PEO−PBT interphase. Therefore, block copolymers with a better phase separation between the PEO phase and the PBT phase show a higher CO_2/He selectivity.

1. Introduction

Poly(ethylene oxide) (PEO) based multiblock copolymers are interesting membrane materials for gas-separation applications because they combine a high polar/(or quadrupolar)/nonpolar gas selectivity with a high permeability.[1] Applications can be found in the acid gas removal from natural gas,[2] removal of CO_2 from gas mixtures in fuel cells, recovery of CO_2 from flue gases, the drying of natural gas[3] and compressed air.

Various PEOs containing block copolymers were studied for their gas-transport properties, which differ in the type of hard segment and the amount of PEO.[1,4−7] These block copolymers consist of two different segments: a hard rigid semicrystalline segment and a soft flexible amorphous PEO segment.

An example of a PEO block copolymer is Pebax, which is a commercially available block copolymer containing hard polyamide domains and soft poly(tetramethylene oxide) (PTMO) or poly(ethylene oxide) (PEO) segments.[1,5,6] Although the gas permeabilities for Pebax-containing PTMO are larger than the ones containing PEO, the polar/nonpolar gas selectivity for the latter is higher, resulting from a strong affinity of the polar ether groups for polar gases.[7]

The gas permeability increases with an increase of the PEO segment length as found for poly(ethylene oxide)−poly(imide) (PEO−PI) block copolymers[4] and polyurethane networks.[8] Morphologies of such block copolymers are very complex, comprising more than only the amorphous and crystalline phase of the blocks but also interphases between them. Such interphases may be of importance for the mass-transport properties, and one desires to have materials at hand which allow systematic variations of the block length, for instance, at constant weight ratio of soft and hard segment. Barbi et al.[6] describe a detailed study elucidating the complex morphology by SAXS as well as relating the gas-transport properties to the morphology. However, the authors used commercially available block copolymers, preventing a systematic study of, for instance, block-length variation at constant amount of soft segment or variation of the amount of soft segment at constant soft segment length. This study addresses exactly this question.

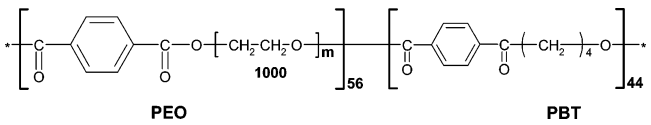

Figure 1. Schematic chemical structure of a PEO−PBT block copolymer carrying the abbreviation 1000PEO56PBT44.

Poly(ethylene oxide) poly(butylene terephthalate) (PEO−PBT) multiblock copolymers allow for such a structural modification through the variation of the PEO segment length and amount of PEO. This enables a systematic study of the relation between the polymeric structure and the gas-transport properties. These polymers have already been investigated for use in medical applications (protein delivery systems,[9] as a skin substitute,[10] none loading bone replacement)[11] or as breathable clothing in textile applications.[12] Gas-transport properties such as permeability, diffusivity, and solubility have not been reported yet.

Figure 1 shows the chemical structure of a typical PEO−PBT block copolymer. PBT forms the hard hy-

* To whom correspondence should be addressed. Phone: +31 53 489 2951. Fax: +31 53 489 4611. E-mail: M.Wessling@utwente.nl.

10.1021/ma049847w CCC: $27.50
Published on Web 05/21/2004

drophobic rigid crystalline phase: PEO forms the soft hydrophilic amorphous rubbery PEO segment. The mechanical and gas-transport properties of these block copolymers can be tailored during polymer synthesis by altering the molecular weight of PEO and the amount of PBT. The following notation classifies the various block copolymers: *m*PEO*y*PBT*x*, where *m* is the molecular weight of the PEO segment (g/mol) and *y* and *x* are the weight percentage of PEO and PBT phase. Figure 1 shows an example of 1000PEO56PBT44, which has a PEO segment length of 1000 g/mol and contains 44 wt % PBT. Depending on the composition of the block copolymer, up to five different phases may be present: two amorphous (PEO and PBT), two crystalline (PEO and PBT), and an interphase in which amorphous PBT is mixed with amorphous PEO.[13]

In this work we study the gas-permeation and thermal properties of PEO−PBT block copolymers. Our aim is to investigate how the permeability of various gases through PEO−PBT block copolymers is affected by the structure of the block copolymer. We want to establish a structure−property relationship for this class of block copolymers and present the following.

(1) The permeability and thermal properties of PEO−PBT block copolymers with a constant segment length but with various amounts of PBT. In particular, we study the effect of the amount of PBT on the solubility and diffusivity of CO_2 and on the tortuosity and chain flexibility of the PEO phase.

(2) The effects of the PEO segment length on the permeability at constant PEO−PBT ratio.

(3) The effect of polymeric composition on the CO_2/N_2 and CO_2/He selectivity.

(4) Finally, the effect of the melting temperature and the degree of crystallinity of the PEO phase on the permeability.

2. Background

The PEO−PBT block copolymers are semicrystalline polymers with the amorphous phase being responsible for most of the gas transport. In this part we describe the approaches used in the literature to quantify the gas transport in semicrystalline materials and in polymers with impermeable fillers.

2.1. Permeability. Following Fick's first law and relating the gas-phase pressure to the concentration inside the polymer through a thermodynamic relationship, such as Henry's law, one can easily derive eq 1, which describes the flux of a gas through a membrane, resulting from a pressure difference over the membrane

$$J = \frac{P}{l}\Delta p \tag{1}$$

where J is the gas flux through the membrane (cm^3(STP)/(cm^2 s)), P the permeability coefficient (Barrer, 1 Barrer = 1×10^{-10} cm^3 (STP)cm/(cm^2 s cmHg)), l the membrane thickness (cm), and Δp the pressure difference over the membrane (cmHg).

The gas permeability of a dense nonporous polymeric material is given as the product of diffusivity and solubility

$$P = DS \tag{2}$$

where D is the diffusivity (cm^2/s) and S the solubility coefficient (cm^3(STP)/(cm^3 polymer cmHg)) of the solute.

PEO−PBT block copolymers consist of two segments, which can be either amorphous or crystalline. The solubility in semicrystalline materials depends on the fraction of amorphous material present in the polymer[14]

$$S = \alpha S_0 \tag{3}$$

where S is the solubility coefficient, α the fraction of amorphous material, and S_0 the solubility coefficient (cm^3(STP)/(cm^3 PEO cmHg)) of a completely amorphous material. Equation 3 implies that the solubility in the crystalline phase can be neglected. In the ideal case, S_0 is independent of pressure. In the case of glassy polymers, S_0 may depend on pressure, showing a concave sorption isotherm; for rubbery polymers and low pressures, S_0 is pressure-independent following Henry's law.

The measured or apparent diffusivity of a solute through a semicrystalline material depends on (1) the tortuosity in the material (τ), which increases with an increased number of impermeable objects, and (2) the chain mobility, which may be reduced at the surface of crystallites. An increase of the tortuosity and lower chain mobility reduce the diffusivity through the amorphous phase following[15]

$$D = \frac{D_0}{\tau\beta} \tag{4}$$

where D is the apparent diffusivity through the block copolymer, D_0 the diffusivity through a completely amorphous material, and β a chain immobilization factor, which increases as the mobility of a chain is reduced. The permeability through semicrystalline materials can be calculated by combining eqs 2−4, resulting in

$$P = \frac{\alpha S_0 D_0}{\tau\beta} \tag{5}$$

PEO−PBT block copolymers comprise a highly permeable PEO phase and a less permeable PBT phase. This PBT phase can be considered as an impermeable obstacle which influences transport through the PEO phase. The Maxwell model describes the gas transport through polymers with noninteracting barriers and can also be used to describe the gas transport in block copolymers[16−19]

$$P_{\text{Maxwell}} = P_0\left(\frac{1-\phi_b}{1+\frac{\phi_b}{2}}\right) \tag{6}$$

where P_0 is the permeability through a completely amorphous material and ϕ_b the volume fraction barrier material. The reduced permeability resulting from the presence of impermeable barriers stems from an increased path length and a reduced cross-sectional area for diffusion. The Maxwell model offers an estimate of the change of diffusivity through the continuous phase due to the presence of randomly dispersed barriers. Equation 6 also assumes that the presence of an impermeable object does not affect the chain mobility of the permeable phase. The Maxwell model is valid for a randomly mixed dispersion of isometric particles with uniform interparticle spacing. The size and shape of the isometric particles is unimportant under the condition

Table 1. Thermal Properties of the PEO−PBT Block Copolymers Used in This Study[a]

	polymer		PEO phase			PBT phase	
	M_x PEO	ratio PEO−PBT	T_g (°C)	T_m (°C)	X_c	T_m (°C)	X_c
		40−60	−46.2	n.d.	n.d.	190.8	0.23
		52−48	−47.5	−10.5	0.05	163.0	0.12
Table 1a	1000	56−44	−48.0	−10.2	0.06	150.6	0.15
		64−36	−49.4	−4.0	0.14	n.d.	n.d.
		75−25	−49.5	7.5	0.20	n.d.	n.d.
	1000		−47.5	−10.5	0.05	163.0	0.12
Table 1b	2000	52−48	−52.5	6.9	0.20	182.7	0.15
	3000		−53.0	19.5	0.26	193.5	0.15
	1000		−49.5	7.5	0.20	n.d.	n.d.
Table 1c	2000	75−25	n.d.	29.6	0.23	n.d.	n.d.
	4000		n.d.	38.6	0.42	n.d.	n.d.
	600		−30.7	n.d.	n.d.	178.8	0.18
Table 1d		40−60					
	1000		-46.2	n.d.	n.d.	190.8	0.23

[a] n.d. = not detected.

that the particles are well separated and that the particle size is in the microscopic range.[18] The nonrandom packing of the impermeable objects can cause deviations from the Maxwell model. The latter may be neglected for block copolymers and polymer blends since these are considered to be randomly mixed.[18] The presence of oriented lamellae in the crystalline phase may affect the permeation properties as well.[19] However, in PEO−PBT block copolymers the PBT phase forms lamellae, which evolve into isotropic spherulites.[12]

3. Experimental Section

3.1. Materials. PEO−PBT block copolymers were obtained from Isotis b.v. (The Netherlands) and used without further purification. Chloroform ($CHCl_3$) and trifluoroacetic acid (TFA) were purchased from Merck (analytical grade) and used as solvents. For the gas-permeation experiments, carbon dioxide (CO_2), nitrogen (N_2), and helium (He) were purchased from Hoekloos b.v. (Netherlands) and methane (CH_4), propane (C_3H_8), and butane (C_4H_{10}) from Praxair n.v. (Belgium). All gases had a purity greater than 99.9%.

3.2. Film Preparation. PEO−PBT block copolymers were dissolved in $CHCl_3$ (5−10 wt %), and TFA was added (±4 vol. % in $CHCl_3$) when the weight ratio of PEO in the block copolymer was lower than 50 wt %. Films of ca. 50 μm were prepared by solution casting on a glass plate. The cast films were dried in a N_2 atmosphere at room temperature for 24 h. The homogeneous dense films were removed from the glass plate and further dried and stored in a vacuum oven at 30 °C.

3.3. Proton NMR. Proton NMR measurements were performed to determine the exact weight ratio between the soft PEO and hard PBT phase as described by Fakirov.[20] The PEO−PBT manufacturer (Isotis b.v.) determined the molecular weight of the PEO segment.

3.4. Differential Scanning Calometry (DSC). The thermal properties of the PEO−PBT block copolymers were determined using a DSC7 (Perkin-Elmer). Indium and cyclohexane were used for calibration. The amount of polymer used was 5−10 mg. The samples were dried in a vacuum oven at 30 °C, and a dry N_2 atmosphere was used in the DSC experiments, preventing water vapor from affecting the measurements. The thermal properties were determined from the second heating scan (heating rate of 10°C/min) in the temperature range from −80 to +250 °C. The glass-transition temperature was determined from the midpoint of the heat capacity change and the melting temperature from the onset of melting.

The degree of crystallinity in both the PEO and PBT phase was calculated by using eq 7

$$X_c = \frac{\Delta H_f}{w\Delta H_f^0} \tag{7}$$

where ΔH_f is the enthalpy of formation of the crystalline PEO or PBT phase (J/g), ΔH_f^0 the enthalpy of formation of the pure crystal (for PEO 144.5 J/g[21] and for PBT 213.4 J/g[20]), and w the weight percent PEO or PBT present in the block copolymer.

3.5. Gas Permeation. Pure gas-permeation properties of the PEO−PBT block copolymer were determined with CO_2, N_2, He, CH_4, and C_3H_8 in the temperature range from 10 to 80 °C. The experiments were performed following the constant-volume variable-pressure method, described in detail elsewhere.[22] Permeabilities were determined at least 8 h after contacting the polymeric film with the gas. Experiments performed on two different membranes yielded values within an experimental error range of 15%. This falls within the systematic error for the characterization equipment used.

3.6. Equilibrium Sorption. Equilibrium sorption of CO_2 in various PEO−PBT block copolymers was obtained for pressures up to 50 bar at 25 °C. The equipment used and the experimental procedure of the sorption measurement are described in detail elsewhere.[23] The obtained sorption isotherms increased linear with pressure following Henry's law

$$C_p = Sp \tag{8}$$

where C_p is the concentration of CO_2 in the block copolymer (cm^3(STP)/cm^3 polymer), S the solubility coefficient (cm^3(STP)/(cm^3(polymer) cmHg)), and p the pressure (cmHg).

4. Results and Discussion

4.1. Thermal Properties of PEO−PBT Block Copolymers. The thermal properties as a function of the chemical structure of the PEO−PBT block copolymer composition were investigated with DSC. Table 1 shows the glass-transition temperature (T_g), melting temperature (T_m), and degree of crystallinity (X_c) of both the PEO and PBT phase of the investigated PEO−PBT block copolymers. The amorphous PBT phases are too small to detect a glass-transition temperature. From the literature it is known that the glass-transition temperature of the PBT phase is located at 55−56 °C and is independent of the composition of the block copolymer.[20]

Up to five different phases can be expected in PEO−PBT block copolymers: two crystalline and two amor-

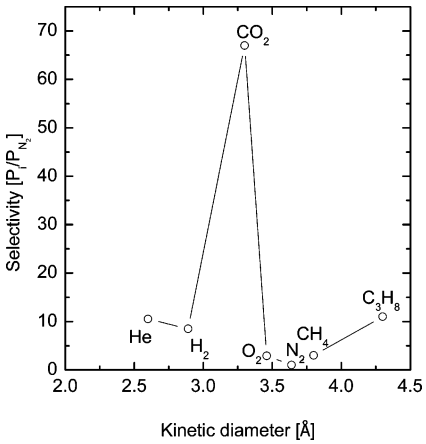

Figure 2. Selectivity for various gases compared to nitrogen at $T = 20$ °C for 1000PEO56PBT44 as a function of the kinetic gas diameter.

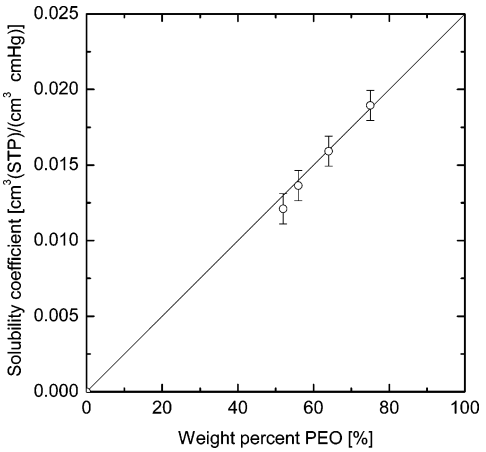

Figure 3. Solubility coefficient of CO_2 at 25 °C for various PEO−PBT block copolymers with a PEO segment of 1000 g/mol. (Open symbols represent experimental values; the line represents results calculated with eq 3 with $S_0 = 0.025$ cm^3(STP)/(cm^3 PEO cmHg)).

phous phases (both PEO and PBT) and an interphase, where amorphous PBT is mixed with amorphous PEO.[13] The presence of the interphase affects the glass-transition temperature of the PEO phase, which increases with increasing amounts of PBT mixed with amorphous PEO.[20] We suggest the amorphous PBT present in the amorphous PEO reduces its chain mobility, thereby increasing the glass-transition temperature of the PEO phase with increasing amounts of PBT.

An increase of the amount of PEO, at the same PEO segment length (Table 1, entry Table 1a), has the following effects on the thermal properties.

(1) The glass-transition temperature of the PEO phase decreases, due to less amorphous PBT present in the amorphous PEO phase.

(2) The melting temperature and the degree of crystallinity of the PEO phase increase due to larger and more regular PEO crystals.

(3) The melting temperature and the degree of crystallinity of the PBT phase show an opposite behavior due to less PBT present in the block copolymer.

Increasing the PEO segment length, at a constant ratio of PEO−PBT, affects the thermal properties in the following way.

(1) The glass-transition temperature of the PEO phase decreases due to a better phase separation between the PEO and PBT phase[24] (Table 1, entries Table 1b and Table 1d).

(2) The melting temperature and the degree of crystallinity of the PEO phase increase due to larger and more regular PEO crystals (Table 1, entries Table 1b and Table 1c).

(3) The melting temperature and the degree of crystallinity of the PBT phase increase due to longer PBT segments (Table 1, entry Table 1b).

These properties must be kept in mind when the gas-transport properties are discussed in the following paragraphs. We point out that most of the permeation experiments are carried out well above the melting temperature of the PEO-crystals.

4.2. Selectivity. Figure 2 shows the gas pair selectivities of various gases compared to N_2 for 1000PEO-56PBT44 as a function of the kinetic diameter[25] of the penetrant. The selectivity decreases with increasing kinetic diameter going from He to N_2. This decrease stems from a lower permeability for the larger molecules[26] caused by a reduced diffusivity. An exception is CO_2, which shows a significantly higher selectivity, caused by a higher solubility for CO_2 due to the strong affinity of the polar ether for polar (or quadrupolar) gases.[7] The selectivity increases for molecules larger than N_2 due to a higher solubility for larger gas molecules.[27] The selectivity values depicted in Figure 2 are only valid for 1000PEO56PBT44 and depend on the polymeric structure, as we will show later.

4.3. Effect of the Amount of PBT on Permeation Properties. This paragraph focuses on the effect of the amount of PBT on the gas-permeation properties of PEO−PBT block copolymers with a PEO segment length of 1000 g/mol. The solubility, diffusivity, and permeability of polar components are significantly affected by the amount of PEO present in the block copolymer.[1] Figure 3 shows the solubility of CO_2 in PEO−PBT block copolymers with a PEO segment length of 1000 g/mol. The error in the solubility coefficient is determined by the least-squares fit of the solubility coefficient when the concentration of CO_2 is plotted versus the pressure (eq 3). (All measured sorption isotherms, concentration as a function of pressure, are linear over the pressure range measured). The slope of the line in Figure 3 represents the weight % normalized solubility coefficient of CO_2 in complete amorphous PEO with a molecular weight of 1000 g/mol. This line is calculated using eq 3 with $S_0 = 0.025$ cm^3(STP)/(cm^3 PEO cmHg). When this line is extrapolated to 0 wt % PEO, no CO_2 sorption is found. This indicates that the solubility of CO_2 in amorphous PBT phase is negligible compared to the solubility in the amorphous PEO phase. The linear increase of the solubility of CO_2 with the amount of PEO also indicates that the solubility of CO_2 in the amorphous PEO phase is not affected by the amount or crystallinity of the PBT phase. Such a behavior is also observed for the solubility of various gases in semicrystalline poly(ethylene).[14]

Figure 4 shows the CO_2 and N_2 permeabilities at 25 °C for various PEO−PBT block copolymers with a PEO segment of 1000 g/mol but with various amounts of PBT as a function of the volume fraction of amorphous PEO. The densities of the amorphous PEO and PBT and crystalline PBT[13] are used to convert the weight % to volume fraction. The permeability of both N_2 and CO_2 increase with the amount of PEO present in the block copolymer. The Maxwell model (eq 6) is used to fit the experimental values of the CO_2 and N_2 permeability of

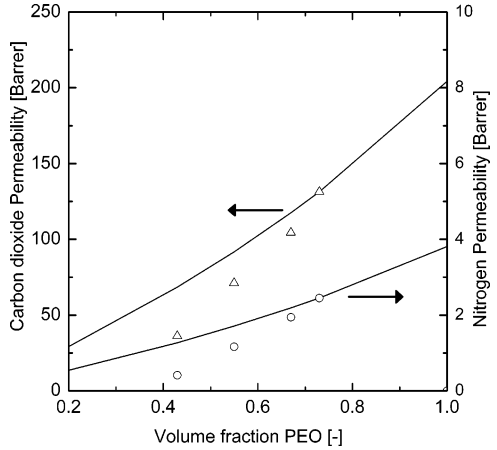

Figure 4. CO_2 (Δ) and N_2 (○) permeability at 25 °C for PEO−PBT block copolymers with a PEO segment length of 1000 g/mol but with various amounts of PEO. (Symbols represent experimental values; lines are calculated with the Maxwell model, eq 6, with $P_0 = 204.3$ Barrer for CO_2 and 3.8 Barrer for N_2).

1000PEO75PBT25 by adjusting P_0, and the result of this fit is presented as lines in Figure 4. The PBT phase is considered to be impermeable for CO_2 and N_2 since the solubility of CO_2 mainly occurs in the amorphous PEO phase (Figure 3). 1000PEO75PBT25 is used for the determination of P_0 in the Maxwell model since this polymer represents the characteristics of pure PEO due to its very high amount of PEO. The results of the Maxwell model, with $P_{0,N2} = 3.8$ Barrer and $P_{0,CO2} = 204.3$ Barrer, are drawn as lines in Figure 4.

The Maxwell model deviates, at lower amounts of PEO considerably, from the experimental values. Deviations between the experimental values and the Maxwell model arise when model assumptions are not completely applicable to the experimental values. The Maxwell model assumes rigid impermeable objects embedded in a permeable PEO phase. However, intermixing of amorphous PBT in the amorphous PEO phase reduces the chain mobility of the PEO phase.[13] This is reflected in the glass-transition temperature of the PEO phase, which increases with an increase of PBT content (Table 1, entry Table 1a). It is also observed for Pebax[6] and polyurethane[8] membranes that imperfect phase separation hampers diffusion and lowers the permeability. This occurs also in PEO−PBT block copolymers where a higher amount of PEO results in a PEO phase with less intermixed amorphous PBT mixed in this phase. The degree of phase separation between the PEO and PBT phase weakens at higher amounts of PBT, causing lower chain mobility and larger deviations between the experimental values and the Maxwell model.

The Maxwell model predicts permeabilities when the mobility of the amorphous phase is not reduced by the presence of impermeable barriers. According to eq 5, using $\beta = 1$, this gives

$$P_{\text{Maxwell}} = \frac{\alpha S_0 D_0}{\tau} \tag{9}$$

However, the chain mobility of the PEO phase is affected by the presence of an impermeable phase. The chain immobilization factor (β) can now be estimated by comparing the measured permeability (eq 5) with the

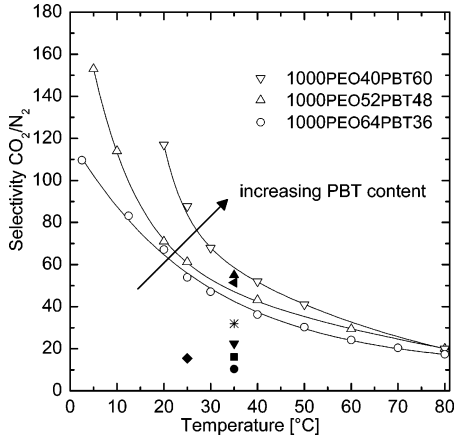

Figure 5. CO_2/N_2 selectivity for various PEO−PBT block copolymers in the temperature range 0−80 °C (○ 1000PEO64-PBT36, △ 1000PEO52PBT48, and ▽ 1000PEO40PBT60). The closed symbols represent literature values (● = PDMS,[32] ■ = poly(phenylene oxide),[32] ▼ = poly(sulfone) and poly(carbonate),[32] * = cellulose acetate,[32] ◆ = natural rubber,[32] triangle left solid PEO−polyamide block copolymer (Pebax1074[1]), ▲ = PEO−PI block copolymer[4]).

Table 2. Chain Immobilization Factor (β) and Tortuosity (τ) Calculated for Various PEO−PBT Block Copolymers with Various Amounts of PEO but with a Constant PEO Segment Length (1000 g/mol)

M_w PEO (g/mol)	ratio PEO-PBT	β	τ
1000	40−60	1.89	1.29
	52−48	1.29	1.23
	64−36	1.13	1.17
	74−25	1.00	1.14

permeability calculated with the Maxwell permeability (eq 9) by taking the ratio of the two

$$\frac{P_{\text{Maxwell}}}{P_{\text{measured}}} = \frac{\left(\frac{\alpha S_0 D_0}{\tau}\right)}{\left(\frac{\alpha S_0 D_0}{\tau\beta}\right)} = \beta \tag{10}$$

The diffusivity through complete amorphous PEO (D_0) is calculated with eq 2 since the permeability and solubility of CO_2 in completely amorphous PEO are known ($P_0 = 204.3$ (Barrer, estimated from 1000PEO75-PBT25), $S_0 = 0.025$ (cm^3(STP)/(cm^3 PEO cmHg)). This gives $D_0 = 8.2 \times 10^{-7}$ (cm^2/s)).

Table 2 shows the chain immobilization factor (β) calculated with eq 10 and the tortuosity (τ) calculated using eq 4. The chain immobilization factor and the tortuosity increase at higher PBT contents, resulting in lower permeability at higher PBT contents as calculated with the Maxwell equation.

Due to the presence of the PEO blocks, PEO-based block copolymers have remarkably high selectivities of CO_2/N_2, for example. Figure 5 shows the CO_2/N_2 selectivity for various PEO−PBT block copolymers in the temperature range 3−80°C and literature values for various polymers (closed symbols). Figure 5 also shows the CO_2/N_2 selectivity for various PEO-based block copolymers with different types of hard segment. In general, one can conclude that PEO-containing block copolymers show a significantly higher selectivity, stemming from the high affinity of the PEO segment for polar components.[1] The order of magnitude of the CO_2/N_2 selectivity at 35 °C is comparable to other PEO-containing block copolymers, indicating that the type

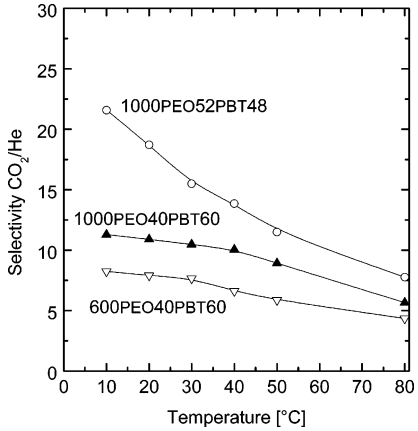

Figure 6. CO_2/He selectivity for 600PEO40PBT60 (▽),1000PEO40PBT60 (▲), and 1000PEO52PBT48 (○) in the temperature range 10−80 °C.

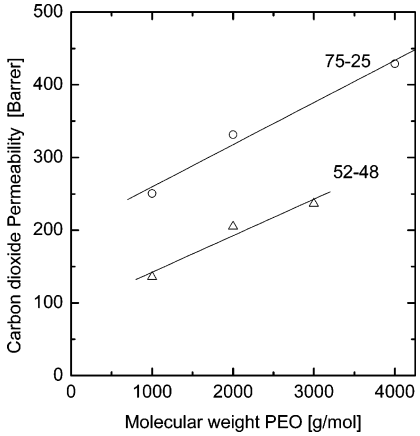

Figure 7. CO_2 permeability at 50 °C of various PEO−PBT block copolymers with PEO−PBT ratio 52−48 (△) and 75−25 (○) with various PEO segment lengths (lines are drawn to guide the eye).

of hard segment contributes to a lesser extent to the selective transport. However, the extent of phase separation still influences the absolute value. The CO_2/N_2 selectivity increases with an increase of the amount of PBT, whereas the CO_2 solubility in the PEO phase at constant PEO block length is not affected by the amount of PBT (Figure 3). This increase in permselectivity must be attributed to differences in diffusion rates of CO_2 and N_2. An increase in the amount of PBT causes a less pronounced phase separation between the PEO and PBT phase. This affects the diffusion rate of the larger N_2 molecule more than CO_2, thereby increasing the selectivity for CO_2/N_2 at higher amounts of PBT.

The CO_2/He selectivity shows a different dependence on the polymeric structure. Figure 6 shows the CO_2/He selectivity for three different PEO−PBT block copolymers as a function of temperature. This figure shows an opposite behavior of the selectivity compared to the CO_2/N_2 selectivity. The block copolymer with the highest amount of PBT (600PEO40PBT60) has the lowest selectivity, whereas an increase of the amount of PEO and the PEO segment length results in a higher selectivity. An increase of the PEO segment length results in a better phase separation between the PEO and PBT phase (compare 600PEO40PBT60 with 1000-PEO40PBT60), reflected in a lower glass-transition temperature for the amorphous PEO phase (Table 1, entry Table 1d). This causes a higher CO_2 permeability due to an increased flexibility of the PEO phase, which favors the diffusivity of CO_2. The dependence of the CO_2/He selectivity on the polymeric structure can be explained by the preferential permeation of CO_2 through the PEO, whereas He diffuses through both the PEO and the mixed PEO−PBT interphase. A less pronounced phase separation between the PEO and PBT phase results in a lower CO_2/He selectivity.

4.4. Effect of PEO Segment Length on Permeation Properties. Not only the amount of PEO but also the PEO segment length influences the thermal and transport properties of PEO−PBT block copolymers. Figure 7 shows the CO_2 permeability at 50 °C for the block copolymers in Table 1 (entries Table 1b and Table 1c). The PEO segment length does not significantly affect the CO_2/N_2 selectivity of these polymers. The permeability in Figure 7 is depicted at 50 °C, since the PEO phase of all the PEO−PBT block copolymers is amorphous at this temperature. The CO_2 permeability increases with an increase of the PEO segment length, which can be caused by an increased diffusivity or an increased solubility of CO_2 in the PEO phase. Table 3 shows the permeability, solubility, diffusivity, and chain flexibility for CO_2 for a series of PEO−PBT block copolymers with a weight ratio PEO−PBT 52−48 but with various PEO segment lengths. The permeability and solubility of 3000PEO52PBT48 are determined by extrapolation from temperatures >40 °C, since the PEO part is completely amorphous at these temperatures. The chain immobilization factor and tortuosity factor of 1000PEO52PBT48 (Table 2) are used for estimation of the chain immobilization factor β (eq 5) for 2000-PEO52PBT48 and 3000PEO52PBT48. Increasing the PEO block length results in a better phase separation having less PBT incorporated in the PEO phase. Since PBT is less mobile than PEO, chain immobilization factors decrease with increasing degree of phase separation (longer PEO blocks), and hence, they can be even below unity with respect to the reference polymer 1000PEO52PBT48. Since these block copolymers contain the same amount of PBT (48 wt %), it is assumed that the tortuosity for diffusion through the materials is equal. The solubility of CO_2 increases with longer PEO segments. This behavior is also observed for the solubility of water in these materials.[28,29] This increased solubility is caused by a larger configurational freedom of the PEO segment, which favors the solubility of water.[30] The diffusivity of CO_2 through these block copolymers rises with longer PEO segments. This is a result of a larger mobility for PEO segments as calculated with eq 5. Both effects, increase in solubility and diffusivity, cause the permeability to increase with larger PEO segments.

4.5. Effect of Temperature on Permeation Properties. The PEO−PBT block copolymers show a rich spectrum of thermal transitions which may influence the permeation properties. The CO_2 permeability is measured in the temperature range 5−80 °C for 2000PEO52PBT48, 3000PEO52PBT48, and 4000-PEO75PBT25. The results are shown in Figure 8. These polymers differ in melting temperature and degree of crystallinity of the PEO phase, as given in Table 1. The permeability is measured with increasing temperature, starting from 5 up to 80 °C, and the permeance values are constant for at least 8 h. The CO_2 permeability increases significantly as the PEO crystals start to melt. The CO_2 permeability below the melting temperature

Table 3. Permeability, Solubility, Diffusivity, and Chain Immobilization Factor (β) for CO_2 at 25 °C for PEO−PBT Block Copolymers with a Ratio PEO−PBT 52−48 and various molecular weights of PEO

M_w PEO (g/mol)	ratio PEO PBT	permeability (Barrer)	solubility (cm^3(STP)/cm^3 cmHg))	diffusivity (cm^2/s)	β
1000		71.0	0.012 ± 0.001	5.3E-07	1.23
2000	52−48	115.8	0.014 ± 0.001	8.3E-07	0.80
3000		146.0	0.016 ± 0.001	9.1E-07	0.72

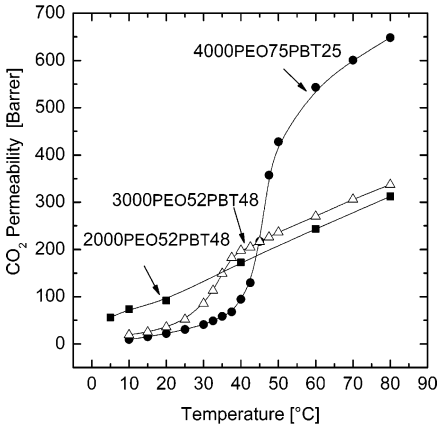

Figure 8. CO_2 permeability for 2000PEO52PBT48 (■),-3000PEO52PBT48 (△), and 4000PEO75PBT25 (◆) in the temperature range 5−80 °C.

of PEO depends on the amount and degree of crystallinity of the PEO phase.

The permeability at 20 °C decreases in the following order $P_{2000PEO52PBT48} > P_{3000PEO52PBT48} > P_{4000PEO75PBT25}$. The permeability of 2000PEO52PBT48 at 20 °C is higher due to the larger amount of amorphous PEO present at 20 °C. The increase in permeance depends on the polymeric structure, which determines the melting temperature and the degree of crystallinity of the PEO phase. 3000PEO52PBT48 and 4000PEO75PBT25 show a gradual increase in permeability when the PEO crystals start to melt. The melting temperature of the PEO phase observed with gas-permeation experiments (Figure 8) does not correspond to the melting temperature as determined with DSC (Table 1) (e.g., 3000PEO52PBT48: $T_{m,DSC} = 19.5$ °C, $T_{m,gaspermeation} = 35$ °C). Deviations between both experiments are caused by (a) different heating rates of the sample and (b) different thermal history. The heating rate in the gas-permeation experiments is much lower (<1 °C/h) compared to the heating rate in DSC experiments (10 °C/min). The low heating rate of the gas-permeation experiments causes the PEO crystals to melt and recrystallize, thereby increasing the melting temperature of PEO. The thermal history of the samples is also very different. The samples analyzed by DSC have been cooled to $T = -80$ °C. The films used for permeation are prepared at room temperature. (Any further cooling may stem from solvent evaporation; however, the extent of cooling is by no means comparable.)

2000PEO52PBT48 does not show a sharp increase in permeability because the PEO phase is still amorphous due to an insufficient temperature gradient to induce crystallization. Similar phenomena are also observed by Hirayama et al.,[31] who observed hysteresis in the increase in permeance between heating and cooling runs.

5. Conclusions

The gas-transport properties of PEO−PBT block copolymers depend on their structure in the following way.

The transport of CO_2 and N_2 occurs mainly through the amorphous PEO phase, whereas He permeates through both the amorphous PEO and the mixed PEO−PBT interphase. This causes the CO_2/He selectivity to decrease with increasing amounts of PBT. The increase of the amount of PBT at constant PEO segment length causes a less pronounced phase separation between the PEO and PBT phase. This lowers the permeability through the amorphous PEO phase more than when the PBT phase is considered as an impermeable barrier obstructing transport.

An increase of the PEO segment length, at the same ratio of PEO−PBT, elevates the chain flexibility of the PEO phase, thereby causing a higher permeance.

The degree of crystallinity and the melting temperature of the amorphous PEO phase, both determined by the amount and PEO segment length, affect the permeance. The melting temperature of the crystalline PEO phase increases with a higher amounts of PEO and longer PEO segments.

Acknowledgment. The European Union is kindly acknowledged for supporting this project: Brite Euram III, Contract no. BRPR-CT 98-0804.[1]

References and Notes

(1) Bondar, V. I.; Freeman, B. D.; Pinnau, I. *J. Polym. Sci., Polym. Phys. Ed.* **2000**, *38*, 2051−2062.
(2) Bhide, B. D.; Voskericyan, A.; Stern, S. A. *J. Membr. Sci.* **1998**, *140*, 27−49.
(3) Metz, S. J.; Potreck, J.; Mulder, M. H. V.; Wessling, M. *Desalination* **2002**, *148*, 303−307.
(4) Okamoto, K.; Fujii, M.; Okamyo, S.; Suzuki, H.; Tanaka, K.; Kita, H. *Macromolecules* **1995**, *28*, 6950−6956.
(5) Kim, J. H.; Ha, S. Y.; Lee, Y. M. *J. Membr. Sci.* **2001**, *190*, 179−193.
(6) Barbi, V.; Funari, S. S.; Gehrke, R.; Scharnagl, N.; Stribeck, N. *Macromolecules* **2003**, *36*, 749−758.
(7) Bondar, V. I.; Freeman, B. D.; Pinnau, I. *J. Polym. Sci., Polym. Phys. Ed.* **1999**, *37*, 2463−2475.
(8) Damain, C. E., E.; Cuney, S.; Pascault, J. P. *J. Appl. Polym. Sci.* **1997**, *65*, 2579−2587.
(9) Bezemer, J. M. R.; Grijpma, R. D. W.; Dijkstra, P. J.; van Blitterswijk, C. A.; Feijen, J. J. *Controlled Release* **2000**, *67*, 249−260.
(10) Beumer, G. J.; Vanblitterswijk, C. A.; Ponec, M. J. *Biomed. Mater. Res.* **1994**, *28*, 545−552.
(11) Radder, A. M.; Leenders, H.; vanBlitterswijk, C. A. *J. Biomed. Mater. Res.* **1996**, *30*, 341−351.
(12) Gebben, B. *J. Membr. Sci.* **1996**, *113*, 323−329.
(13) Fakirov, S.; Apostolov, A. A.; Boeseke, P.; Zachmann, H. G. *J. Macromol. Sci., Phys.* **1990**, *B29*, 379−395.
(14) Michaels, A. S.; Bixler, H. J. *J. Polym. Sci.* **1961**, *50*, 393−412.
(15) Michaels, A. S.; Bixler, H. J. *J. Polym. Sci.* **1961**, *50*, 413−439.
(16) Barrer, R. M. *Diffusion in polymers;* Academic Press: New York, 1968.
(17) Merkel, T. C.; Freeman, B. D.; Spontak, R. J.; He, Z.; Pinnau, I.; Meakin, P.; Hill, A. J. *Science* **2002**, *296*, 519−522.

(18) Petropoulos, J. H. *J. Polym. Sci., Polym. Phys. Ed.* **1985**, *23*, 1309−1324.
(19) Arnold, M. E.; Naga, I. K.; Freeman, B. D.; Spontak, R. J.; Betts, D. E.; DeSimone, J. M.; Pinnau, I. *Macromolecules* **2001**, *34*, 5611−5619.
(20) Fakirov, S.; Gogeva, T. *Makromol. Chem.* **1990**, *191*, 603−614.
(21) Tsutsui, K.; Yoshimizu, H.; Tsujita, Y.; Kinoshita, T. J. *Appl. Polym. Sci.* **1999**, *73*, 2733−2738.
(22) Bos, A.; Punt, I. G. M.; Wessling, M.; Strathmann, H. *J. Polym. Sci., Polym. Phys. Ed.* **1998**, *36*, 1547−1556.
(23) Krause, B.; Sijbesma, H. P.; Munuklu, P.; van der Vegt, N. F. A.; Wessling, M. *Macromolecules* **2001**, *34*, 8792−8801.
(24) Fakirov, S.; Gogeva, T. *Makromol. Chem.* **1990**, *191*, 615−624.
(25) Breck, D. W. *Zeolite molecular sieves: structure, chemistry, and use;* Wiley: New York, 1974.
(26) Koros, W. J.; Hellums, M. W. In *Encyclopedia of polymer science and engineering;* Kroschwitz, J. I., Ed.; Wiley: New York, 1990; pp 724−802.
(27) Mulder, M. H. V. *Basic principles of membrane technology,* 2nd ed.; Kluwer: Dordrecht, 1996.
(28) Bezemer, J. M.; Grijpma, D. W.; Dijkstra, P. J.; van Blitterswijk, C. A.; Feijen, J. *J. Controlled Release* **1999**, *62*, 393−405.
(29) Deschamps, A. A.; Grijpma, D. W.; Feijen, J. *Polymer* **2001**, *42*, 9335−9345.
(30) Metz, S. J.; van der Vegt, N. F. A.; Mulder, M. H. V.; Wessling, M. *J. Phys. Chem. B* **2003**, *107*, 13629−13635.
(31) Hirayama, Y.; Kase, Y.; Tanihara, R.; Sumiyama, Y.; Kusuki, Y.; Haraya, K. J. *Membr. Sci.* **1999**, *160*, 1.
(32) Ho, W. S. W.; Sirkar, K. K. *Membrane Handbook;* Van Nostrand Reinhold: New York, 1992.

MA049847W